Environment International 89–90 (2016) 212–221

Contents lists available at ScienceDirect

Environment International

journal homepage: www.elsevier.com/locate/envint

Status and characteristics of ambient $PM_{2.5}$ pollution in global megacities

Zhen Cheng [a], Lina Luo [a], Shuxiao Wang [b,*], Yungang Wang [c,i], Sumit Sharma [d], Hikari Shimadera [e], Xiaoliang Wang [f], Michael Bressi [g], Regina Maura de Miranda [h], Jingkun Jiang [b], Wei Zhou [b], Oscar Fajardo [b], Naiqiang Yan [a], Jiming Hao [b]

[a] School of Environmental Science and Engineering, Shanghai Jiao Tong University, Shanghai 200240, China
[b] School of Environment, State Key Joint Laboratory of Environment Simulation and Pollution Control, Tsinghua University, Beijing 100084, China
[c] Environmental Energy Technologies Division, Lawrence Berkeley National Laboratory, Berkeley, CA 9472 0, USA
[d] Earth Science and Climate Change Division, The Energy and Resources Institute, IHC complex, Lodi Road, New Delhi-3, India
[e] Graduate School of Engineering, Osaka University, 2-1 Yamada-oka, Suita, Osaka 565-0871, Japan
[f] Division of Atmospheric Sciences, Desert Research Institute, 2215 Raggio Parkway, Reno, NV 89512, USA
[g] European Commission, Joint Research Centre, Institute for Environment and Sustainability, Ispra, VA, Italy
[h] School of Arts, Sciences, and Humanities, University of São Paulo, Rua Arlindo Béttio,1000, Ermelino Matarazzo, CEP 03828-000 São Paulo, Brazil
[i] GAGO Inc., San Jose, CA 95131, USA

ARTICLE INFO

Article history:
Received 14 September 2015
Received in revised form 27 January 2016
Accepted 2 February 2016
Available online xxxx

Keywords:
$PM_{2.5}$ (fine particulate matter)
Megacity
Air pollution
Chemical composition

ABSTRACT

Ambient $PM_{2.5}$ pollution is a substantial threat to public health in global megacities. This paper reviews the $PM_{2.5}$ pollution of 45 global megacities in 2013, based on mass concentration from official monitoring networks and composition data reported in the literature. The results showed that the five most polluted megacities were Delhi, Cairo, Xi'an, Tianjin and Chengdu, all of which had an annual average concentration of $PM_{2.5}$ greater than 89 μg/m^3. The five cleanest megacities were Miami, Toronto, New York, Madrid and Philadelphia, the annual averages of which were less than 10 μg/m^3. Spatial distribution indicated that the highly polluted megacities are concentrated in east-central China and the Indo-Gangetic Plain. Organic matter and SNA (sum of sulfate, nitrate and ammonium) contributed 30% and 36%, respectively, of the average $PM_{2.5}$ mass for all megacities. Notable seasonal variation of $PM_{2.5}$ polluted days was observed, especially for the polluted megacities of China and India, resulting in frequent heavy pollution episodes occurring during more polluted seasons such as winter. Marked differences in $PM_{2.5}$ pollution between developing and developed megacities require more effort on local emissions reduction as well as global cooperation to address the $PM_{2.5}$ pollution of those megacities mainly in Asia.
© 2016 Elsevier Ltd. All rights reserved.

1. Introduction

Ambient fine particulate matter ($PM_{2.5}$) refers to particles with an aerodynamic diameter of less than 2.5 μm. $PM_{2.5}$ has adverse impacts on human health, visibility, ecosystems and climate change (Brauer et al., 2012; Cheng et al., 2013; IPCC, 2013; Kan et al., 2012; Madrigano et al., 2013; Zhang et al., 2012b). These impacts are more notable for global megacities. The agglomerated population of megacities results in a high emission amount of pollutants due to intensive energy consumption (Butler et al., 2008). The elevated concentration of pollutants such as $PM_{2.5}$ will affect substantially more people in megacities than in rural regions (Gurjar et al., 2010). Research on $PM_{2.5}$ pollution has paid more attention to the megacities than other locations, from those in developed countries, such as Tokyo, Paris and Los Angeles, to those in developing countries, such as Beijing, Hong Kong, Mumbai and Santiago (Bressi et al., 2013; Hara et al., 2013; Hasheminassab et al., 2014; Huang et al., 2014a, 2014b; Joseph et al., 2012; Villalobos et al., 2015; Yu et al., 2013). However, most of these studies rely on the measured results from one short episode or at a single site conducted by different groups with different measurement techniques, making it difficult to accurately represent long-term conditions.

Data of $PM_{2.5}$ pollution status on the global scale is scarce. The World Health Organization (WHO) collects and publishes a database on the ambient air pollution in global cities every year (WHO, 2014). The number of covered cities is ample and comprehensive, but the $PM_{2.5}$ concentration is converted from PM_{10} results for many cities of developing countries such as China. Furthermore, no additional data analysis is conducted in the WHO database. Zhang et al. (2012b) compared the integrated mass and species concentration of PM_{10} from Chinese sites with those from other countries or regions, but the Chinese sites are primarily located in rural areas or medium cities and only PM_{10} was included. The $PM_{2.5}$ mass or composition derived from satellite sensor observations such as MODIS and MISR provide another investigation path for global $PM_{2.5}$ distribution (Boys et al., 2014; Philip et al., 2014; van Donkelaar et al., 2015). The disadvantage of this satellite-based method is the significant uncertainties caused by the precision of the

* Corresponding author.
E-mail address: shxwang@tsinghua.edu.cn (S. Wang).

http://dx.doi.org/10.1016/j.envint.2016.02.003
0160-4120/© 2016 Elsevier Ltd. All rights reserved.

inversion algorithm and the adverse meteorological impact on the bias of the detected signal.

A quantitative comparison based on in situ and simultaneous $PM_{2.5}$ observations for global megacities is seldom reported. China added $PM_{2.5}$ to its new national air quality standard in 2012. The execution of the $PM_{2.5}$ monitoring network in China provides the fundamental database for this study. The published $PM_{2.5}$ concentration from the official monitoring network of 45 global megacities for the entire year of 2013 was collected. In addition, the global $PM_{2.5}$ distribution and composition for 2013 from previous studies are also reviewed. We intend to provide a comprehensive review of the current status of the $PM_{2.5}$ mass level, composition, temporal variation and principal causes in global megacities, which will provide substantial support for the assessment of health impacts related to air pollution, as well as strategies for controlling global air pollution.

2. Data sources and methods

2.1. $PM_{2.5}$ mass and processing procedure

A megacity in this study is defined as an urban agglomeration with more than 5 million inhabitants. According to the criteria set forth by the United Nations, there were 71 cities characterized as megacities per the population data from 1 July 2014 (United Nations, 2014). The list of megacities (shown in Fig. 1 and Table S1 of the supplemental materials section) was derived from a published report by the United Nations (United Nations, 2014). These megacities are primarily located in Asia, Europe and North America.

The $PM_{2.5}$ raw datasets from 2013-1-1 to 2013-12-31 were collected and investigated using a website of air quality broadcasting or the periodical air quality report provided by local environmental protection bureaus. There were 45 megacities that had measured and published $PM_{2.5}$ concentration levels, whereas data from the other 26 megacities were unavailable. Web addresses of the data sources are listed in Table S2 of the supplemental materials section. All of the datasets used in this study were confirmed to be from official departments and to have covered a sufficient temporal length of the year 2013. According to the dataset resolution in Table S1, the 26 megacities whose $PM_{2.5}$ data were unavailable were from Asia, Africa and South America, except for Istanbul, in Europe. For the remaining 45 megacities, hourly, daily or 3-day resolutions were obtained for all cities, except Delhi, Cairo and Dhaka. Only the annual average $PM_{2.5}$ for Delhi and Cairo and the monthly average for Dhaka were available for this study.

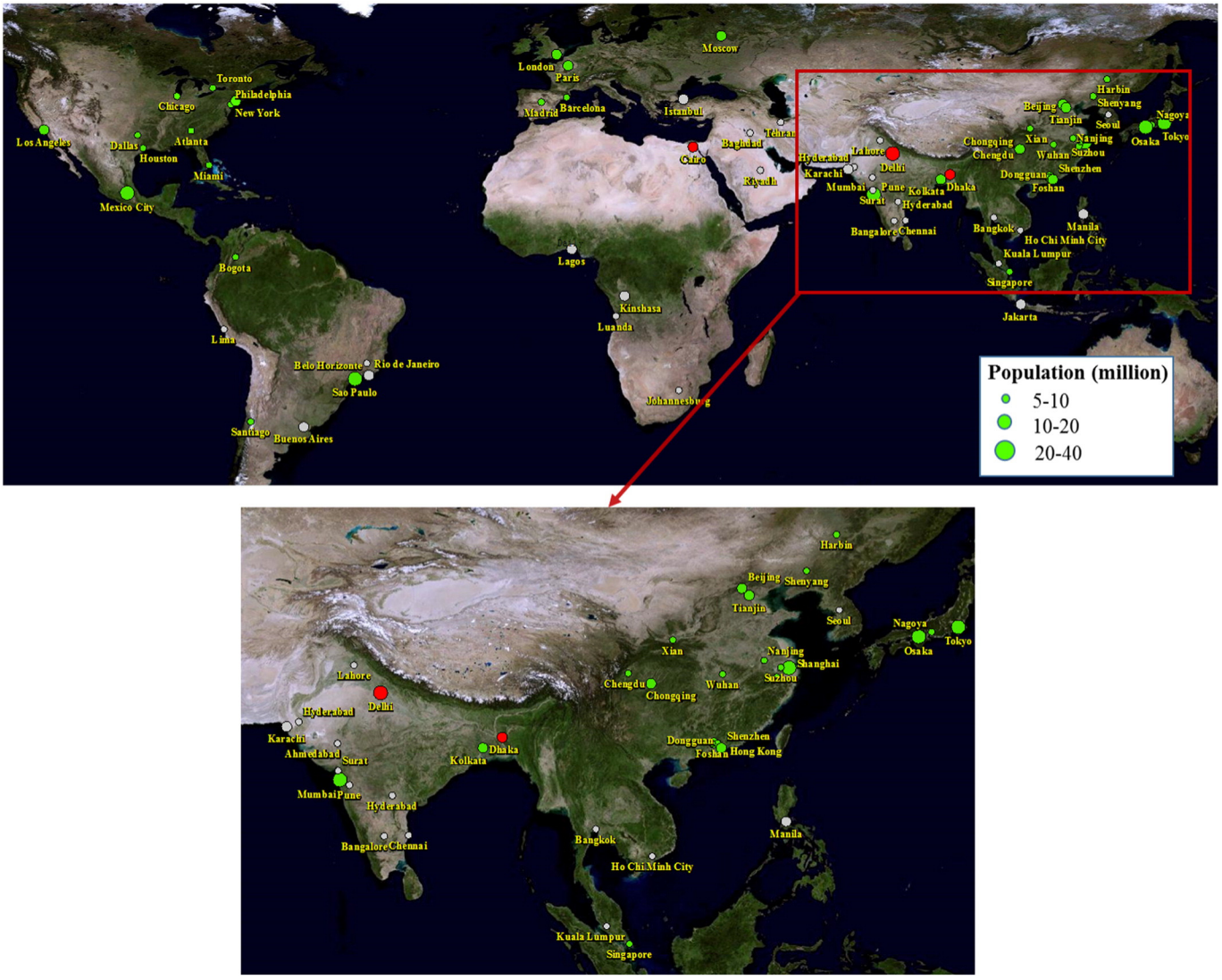

Fig. 1. Global megacities distribution and their availability of $PM_{2.5}$ data. The symbol size used for the megacities represents three classes of population size. The symbol colors represent the data availability of $PM_{2.5}$, i.e., green: hourly or daily or 3-days; red: monthly or annual; grey: not available. (For interpretation of the references to color in this figure legend, the reader is referred to the web version of this article.)

The annual average and polluted days in the different concentration ranges for each megacity were derived from the raw datasets. The raw hourly, daily, 3-day or monthly records were averaged to obtain the annual average for each observation site, then the annual average and its standard deviation value for each megacity were calculated from the corresponding values of all sites in each megacity. To determine the days in the different concentration ranges, the ratio of days in the different concentration ranges was first calculated by dividing the counted days by all sampling days, then multiplying by 365 to obtain the days for each concentration range. Five ranges of $PM_{2.5}$ concentration were divided by the daily threshold values of 25, 37.5, 50 and 75 μg/m^3, according to the WHO's interim targets for the daily concentration (WHO, 2006).

2.2. Satellite-derived product

Satellite-derived $PM_{2.5}$ results were collected to provide the geographic distribution for the area around all the megacities, which might help explain the differences and causes of the spatial diversity of $PM_{2.5}$ pollution in the megacities. The global satellite-derived $PM_{2.5}$ with the resolution of 0.1° * 0.1° in 2010–2012 at a relative humidity of 35%, developed and provided by van Donkelaar et al. (2015), was selected for use in this study.

2.3. $PM_{2.5}$ chemical composition

The concentrations of $PM_{2.5}$ compositions for megacities were collected and processed from the literature whose sampling date was around 2013 and time length was about one year. Organic matter (OC multiplied by 1.4 to represent the mass of C, N, O etc.), elemental carbon (EC), sulfate, nitrate and ammonium (SNA), soil and unidentified were used for the $PM_{2.5}$ mass closure (Chow et al., 2015). "Soil" was calculated from the weighted summation of five major soil elements, i.e., 2.2Al + 2.49Si + 1.63Ca + 2.42Fe + 1.94Ti (Lowenthal and Naresh, 2003). For the unmeasured element, it is estimated by the mass ratio to the measured element of upper continental crust given by Taylor and McLennan (1995). "Unidentified" refers to the remaining mass between the $PM_{2.5}$ mass and the summation of the aforementioned four groups of chemical compositions.

3. Results and discussion

3.1. $PM_{2.5}$ integrated mass concentration

Investigation of the observation sites included a measurement method of the $PM_{2.5}$ mass and the current $PM_{2.5}$ threshold of the air quality standard for each megacity (shown in Table 1). The number of monitoring sites varied from 1 in several US megacities to 45 in Tokyo. The measurement methods of the $PM_{2.5}$ mass include gravimetric, beta attenuation, tapered element oscillating microbalance (TEOM) and TEOM with a filter dynamics measurement system (FDMS). Different methods had their own advantages and disadvantages (Chow et al., 2008). No tendency towards a specific measurement method was observed among the megacities. As to the $PM_{2.5}$ standard, some European megacities (i.e., Paris, London, Madrid and Barcelona) only had an annual (no daily) threshold in their standards. Megacities in the same country usually had the same national standard for annual or daily threshold values. Only Toronto of Canada met the WHO's annual guideline value of 10 μg/m^3, and no megacity met the daily 25 μg/m^3 WHO guideline value. The countries whose threshold was equal to or lower than the WHO's Interim Target-3 values (annual: 15 μg/m^3, daily: 37.5 μg/m^3) included the United States, Canada, Japan and Singapore. Egypt, India and China had the most relaxed annual threshold values of 50, 40 and 35 μg/m^3, respectively. The corresponding daily threshold values for these three countries are 80, 60 and 75 μg/m^3, respectively. The wide gap in the threshold values between developed and developing countries reflected the status and control efforts of $PM_{2.5}$ pollution, also indicating the progress developing countries must make towards attaining the WHO guideline.

By averaging all of the validated raw $PM_{2.5}$ records in 2013, the $PM_{2.5}$ annual concentration is calculated and ranked for all the megacities (shown in Fig. 2). The five most polluted megacities with the highest $PM_{2.5}$ concentrations were Delhi (143.0 ± 17.8), Cairo (109.6 ± 27.7), Xi'an (102.2 ± 9.3), Tianjin (95.7 ± 7.7) and Chengdu (89.4 ± 14.4 μg/m^3). Only Cairo is in Africa, while the other four megacities are in India or China, in Asia. In contrast, the five least polluted megacities were Miami (6.7), Toronto (8.4 ± 0.3), New York (9.1 ± 1.0), Madrid (9.9 ± 1.3) and Philadelphia (10.3 ± 1.0 μg/m^3). Only Madrid, Spain, is in Europe, and the other four megacities are in the United States or Canada, in North America.

According to the annual threshold values of the WHO guideline (WHO, 2006), only four megacities attained the WHO guideline value of 10 μg/m^3; they are referred to as "WHO-attainment" megacities, and their annual concentrations were 6.7–9.9 μg/m^3. Another five megacities, whose concentrations were between 10 μg/m^3 and the interim target III value of 15 μg/m^3, are referred to as "target III-attainment" megacities and their concentrations were 10.3–11.6 μg/m^3. Another 11 megacities are referred to as "target II-attainment" megacities because their concentrations of 15.3–22.4 μg/m^3 are all between 15 μg/m^3 and the interim target II level of 25 μg/m^3. Additional five megacities only attained the interim target I level of 35 μg/m^3 and are referred to as "target I-attainment" megacities, with a concentration of 25.9–30.8 μg/m^3. The remaining 20 megacities, whose concentrations (40.0–143.0 μg/m^3) were all greater than 35 μg/m^3, are referred to as "non-attainment" megacities.

The spatial distribution of $PM_{2.5}$ hotspots between discrete megacities and satellite-derived grids was shown to be consistent at the global scale (shown in Fig. 3). The "non-attainment" megacities concentrated in eastern China and northeast India, as well as Cairo, Egypt, were based on official field measurements, whereas the satellite-derived product presented "non-attainment" regions as covering most areas of east-central China and the Indo-Gangetic Plain (van Donkelaar et al., 2015). The pollution of "non-attainment" megacities in China and India has already become a severe regional problem rather than a local discrete issue. The five "target I-attainment" megacities were Hong Kong, Mumbai, Bogota, Santiago and Mexico City. The former two were probably affected by the regional heavy pollution in China and India, whereas pollution in the latter three megacities was more likely attributed to local urban influence, as indicated by the satellite distribution results. The 11 "target II-attainment" megacities included 4 in Europe, 4 in Japan, Singapore, Sao Paulo and Los Angeles. Satellite distribution indicated that the pollution in most "target II-attainment" megacities occurs at the local scale, only the four megacities in Europe show regional distribution. The four "WHO-attainment" and five "target III-attainment" megacities were all located in North America, except for Madrid, in Europe. In general, the satellite-derived $PM_{2.5}$ had a high correlation with the field direct measurement results, with the correlation coefficient of 0.87, in despite of different temporal coverage and spatial resolution between the two datasets.

The $PM_{2.5}$ spatial diversity between global megacities, indicated by both field measurement and satellite inversion, was mainly related to the emission intensity of anthropogenic pollutants. These pollutants included the primary emission of fine particulate matter, as well as gaseous precursors including sulfur dioxide, oxides of nitrogen, ammonia and volatile organic compounds that could ultimately be oxidized to form particulate matter. China and India were estimated to contribute 35.8% and 13.8% of global anthropogenic $PM_{2.5}$ emissions, respectively, and the emission intensities of eastern China and the Indo-Gangetic Plain were both higher than 10^6 g/km^2-year in 2007 (Huang et al., 2014c). The fuel consumption sectors, such as power plants, industry, residential and commercial buildings, contributed to the dominant primary $PM_{2.5}$ emissions for China and India (Huang et al., 2014c). For

Table 1
Configuration of $PM_{2.5}$ measurements for the megacities in this study.

Country	Megacity	Sites	Measurement method	Ambient standard (μg/m^3)	
				Annual	Daily
USA	Atlanta	1	Gravimetric	12	35
Spain	Barcelona	7	Gravimetric	25	N/A
China	Beijing	12	TEOM-FDMS	35	75
Colombia	Bogota	1	Beta attenuation	25	50
Egypt	Cairo	13	Gravimetric	50	80
China	Chengdu	8	TEOM-FDMS or beta attenuation	35	75
USA	Chicago	4	Gravimetric	12	35
China	Chongqing	16	TEOM-FDMS or beta attenuation	35	75
USA	Dallas	4	Gravimetric or beta attenuation	12	35
India	Delhi	6	Beta attenuation	40	60
Bangladesh	Dhaka	11	Beta attenuation	15	65
China	Dongguan	5	TEOM-FDMS or beta attenuation	35	75
China	Foshan	8	TEOM-FDMS or beta attenuation	35	75
China	Guangzhou	11	TEOM-FDMS	35	75
China	Hangzhou	11	TEOM-FDMS or beta attenuation	35	75
China	Harbin	12	TEOM-FDMS or beta attenuation	35	75
China	Hong Kong	11	TEOM	35	75
USA	Houston	1	Gravimetric	12	35
Japan	Kitakyushu-Fukuoka	2	TEOM or beta attenuation	15	35
India	Kolkata	10	Beta attenuation	40	60
England	London	3	TEOM-FDMS	25	N/A
USA	Los Angeles	4	Beta attenuation	12	35
Spain	Madrid	6	TEOM	25	N/A
Mexico	Mexico City	12	Gravimetric or beta attenuation	12	45
USA	Miami	1	Gravimetric	12	35
Russia	Moscow	2	TEOM	25	35
India	Mumbai	1	Beta attenuation	40	60
Japan	Nagoya	14	TEOM or beta attenuation	15	35
China	Nanjing	9	TEOM-FDMS or beta attenuation	35	75
USA	New York	10	Gravimetric	12	35
Japan	Osaka	42	TEOM or beta attenuation	15	35
France	Paris	9	TEOM-FDMS	25	N/A
USA	Philadelphia	6	Gravimetric or beta attenuation	12	35
Chile	Santiago	11	Beta attenuation	20	50
Brasil	Sao Paulo	4	Beta attenuation	20	60
China	Shanghai	10	TEOM-FDMS	35	75
China	Shenyang	11	TEOM-FDMS or beta attenuation	35	75
China	Shenzhen	11	TEOM-FDMS or beta attenuation	35	75
Singapore	Singapore	5	Beta attenuation	12	37.5
China	Suzhou	8	TEOM-FDMS or beta attenuation	35	75
China	Tianjin	15	TEOM-FDMS or beta attenuation	35	75
Japan	Tokyo	45	TEOM or beta attenuation	15	35
Canada	Toronto	4	TEOM	10	28
China	Wuhan	10	TEOM-FDMS or beta attenuation	35	75
China	Xi'an	13	TEOM-FDMS or beta attenuation	35	75

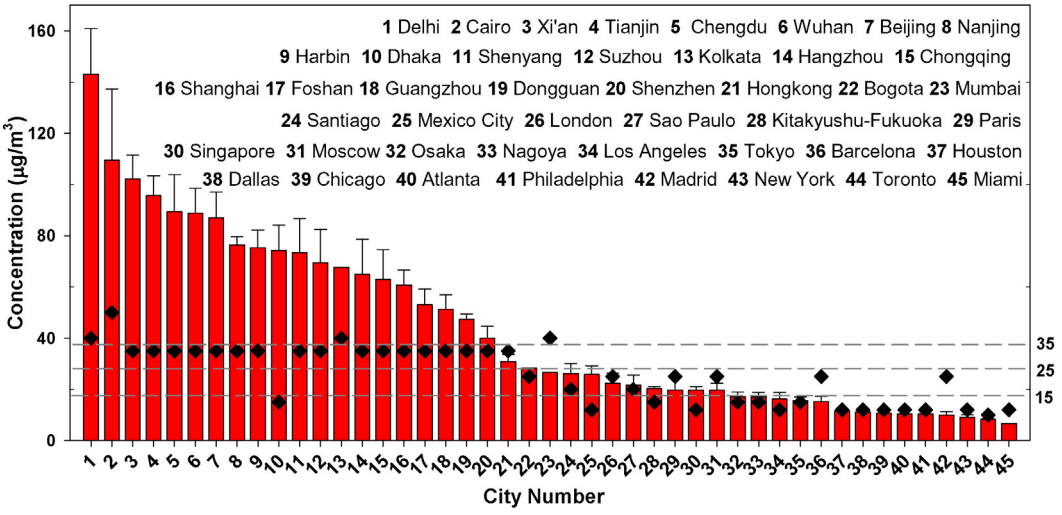

Fig. 2. Annual average $PM_{2.5}$ concentrations of global megacities. The ends of the whiskers represent one standard deviation of the annual average concentration. The numbers 15, 25 and 35 on the right represent the three annual concentration thresholds of the three interim targets of the WHO. The black diamond symbol represents the annual standard for each megacity.

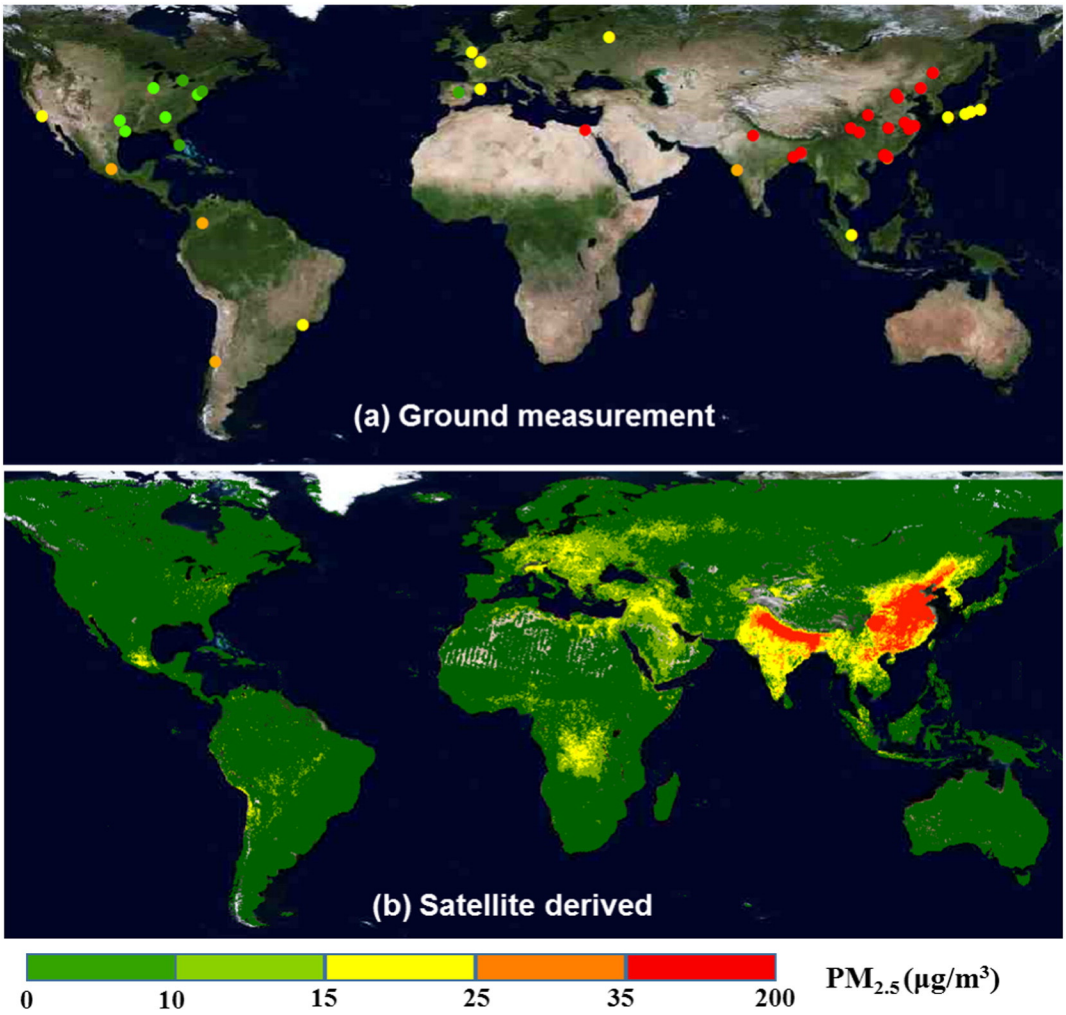

Fig. 3. $PM_{2.5}$ mass comparison between satellite-derived and measured values. The top panel (a) is the ground measurement of the $PM_{2.5}$ annual concentration using the dataset of this study. The bottom panel (b) is the satellite-derived $PM_{2.5}$ annual concentration distribution provided by van Donkelaar et al., 2015 (http://fizz.phys.dal.ca/~atmos/datasets/Unified_PM25_GL_201001_201212-RH35-minc0_Median_NoDust_NoSalt-NoNegs.asc.zip).

example, China and India respectively emitted 29.1% and 10.1% of the global anthropogenic sulfur dioxide in 2011, and the majority of the emissions were concentrated in the polluted regions shown in Fig. 3 (Klimont et al., 2013). Energy-generation and industry are estimated to be the largest sources of sulfur dioxide emissions for both China and India (Klimont et al., 2013). The primary reason for the high emission intensity was due to the continuous industrialization and urbanization of developing countries as well as the increased globalization, specifically the design and service-oriented economies in developed countries contrasted with the energy- and emission-intensive production economies in developing countries (Lin et al., 2014).

3.2. $PM_{2.5}$ chemical composition and source apportionment

Organic matter and SNA were the dominant $PM_{2.5}$ components for global megacities. From the published studies of the $PM_{2.5}$ chemical composition in 38 megacities (shown in Fig. 4), the average percentage of each composition was 30 ± 8% for organic matter (OM), 7 ± 4% for elemental carbon (EC), 36 ± 10% for SNA, 10 ± 5% for soil and 19 ± 12% for unidentified. Organic matter is typically regarded as being half from the primary emission source and half from the oxidation of volatile organic compounds (Day et al., 2015). In addition, SNA are regarded as originating entirely from the oxidation of gaseous precursors such as sulfur dioxide and nitrogen oxides, whereas elemental carbon and soil typically originate from the primary emissions of industry, mobile sources and dust. As a result, 51% of the $PM_{2.5}$ mass for global megacities was estimated to come from a secondary oxidation path, whereas the remaining 49% came from the direct emission of primary sources.

The composition ratios of megacities in this study were comparable with the global population-weighted compositions, which are derived from satellite and chemical transport models (Philip et al., 2014). An organic mass of 30% in megacities was similar to that of 32% in the global population-weighted composition. This is also suitable for the EC, whose fraction is 7% for the two cases. The SNA percentage of 36% for megacities was slightly higher than the 30% for the global population-weighted composition. The major difference was for the soil (mineral dust) contribution. A soil percentage of 30% in the global population-weighted composition is more than triple that of 9% in the global megacities. Because the global population-weighted results include both urban and rural populations, the SNA ratio is reasonably lower than that of the megacities because almost all of the SNA was oxidized from the gaseous pollutants emitted by fossil fuels, which were used more in megacities. In contrast, a notably rural population located in sub-Saharan Africa, with a high soil concentration and without any megacities, resulted in a rather high soil percentage for the global population-weighted composition (Philip et al., 2014; United Nations, 2014).

The diversity of the composition ratio between each megacity was notable. The OM ranged from 16% in Harbin to 53% in Kolkata, and the EC increased from 1% to 20% in the same two megacities. The SNA varied

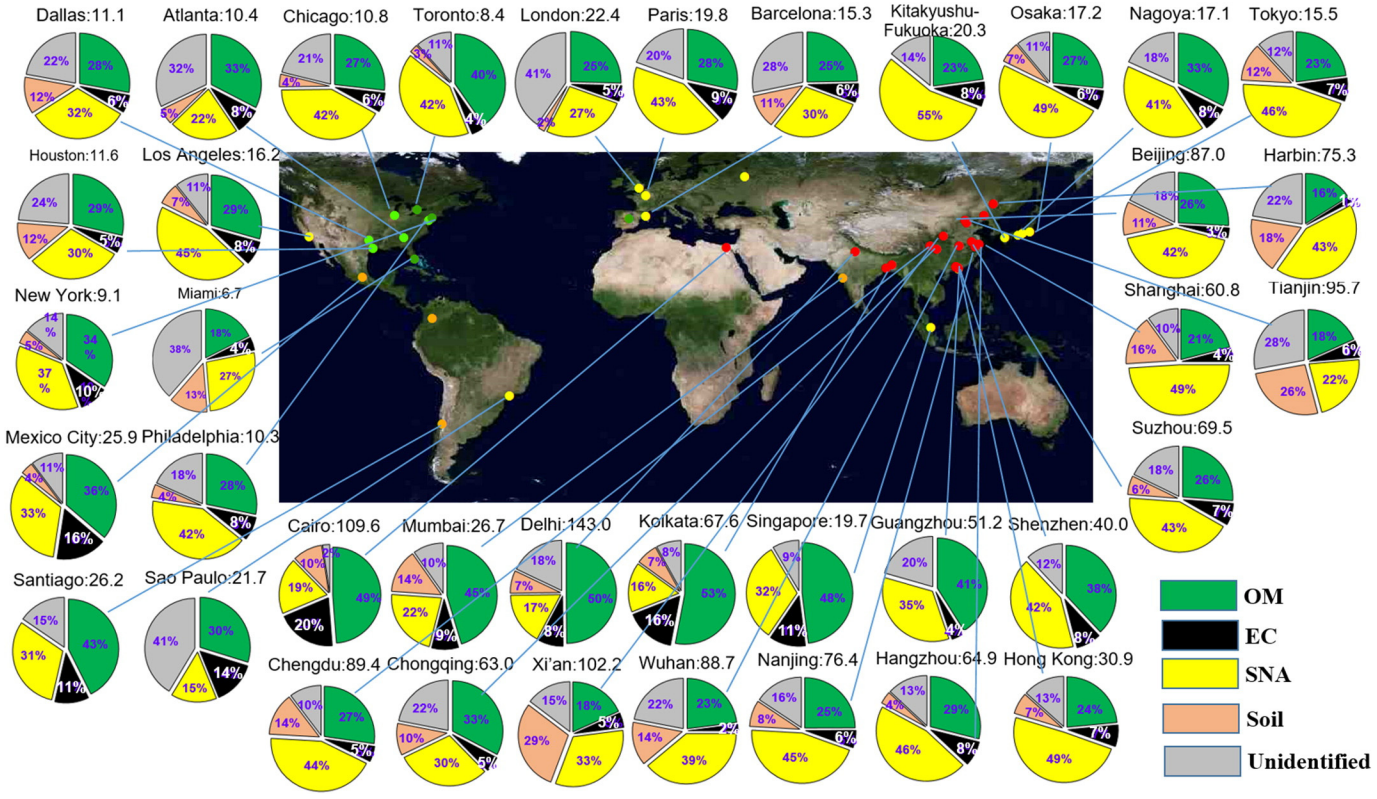

Fig. 4. $PM_{2.5}$ chemical composition for global megacities. The symbol color and number of the megacities represents the measured annual $PM_{2.5}$ concentration in 2013. OM (organic matter) = 1.4 * OC, EC: elemental carbon, SNA: sulfate, nitrate and ammonium, soil = 2.2Al + 2.49Si + 1.63Ca + 2.42Fe + 1.94Ti, unidentified = $PM_{2.5}$ mass–OM–EC–SNA–soil. The chemical compositions of Dhaka, Shenyang, Dongguan, Foshan, Madrid, Bogota and Moscow are unavailable. The sampling date and references for each megacity are as follows: **Atlanta**, 2013, *U.S. EPA chemical speciation network*; **Barcelona**, 2003–2004, *Rodriguez et al., 2007*, EC refers to black carbon here, Sulfate refers to non-sea-salt sulfate; **Beijing**, 2012–2013, *Liu et al., 2015*; **Cairo**, 2010, *Lowenthal et al., 2013*; **Chengdu**, 2012–2013, *Chen et al., 2015b*; **Chicago**, 2013, *U.S. EPA chemical speciation network*; **Chongqing**, 2005–2006, *Yang et al., 2011*; **Dallas**, 2013, *U.S. EPA chemical speciation network*; **Delhi**, 2001–2002, *Chowdhury, 2004*; **Guangzhou**, 2013–2014, *Guangzhou EPB*, No soil data; **Hangzhou**, 2011–2012, *Cheng 2014*; **Harbin**, 2013–2014, *Jia 2014*; **Hong Kong**, 2011–2012, *Huang et al., 2014b*, EC refers to soot concentration; **Houston**, 2013, *U.S. EPA chemical speciation network*; **Kitakyushu-Fukuoka**, 2012–2013, *Ministry of the Environment, Japan, 2014*, No soil data; **Kolkata**, 2001–2002, *Chowdhury, 2004*; **London**, 2004–2005, Rodriguez et al., 2007, EC refers to black carbon here, Sulfate refers to non-sea-salt sulfate; **Los Angeles**, 2013, *U.S. EPA chemical speciation network*; **Mexico City**, 2003–2004, *Vega et al., 2011*, Ti is calculated by [Al]/26.8; **Miami**, 2013, *U.S. EPA chemical speciation network*; **Mumbai**, 2007–2008, *Joseph et al., 2012*; **Nagoya**, 2012–2013, *Ministry of the Environment, Japan, 2014*, No soil data; **Nanjing**, 2011–2012, *Chen et al., 2015a*, Ti is calculated by [Al]/26.8; **New York**, 2013, *U.S. EPA chemical speciation network*, Ti is calculated by [Al]/26.8; **Osaka**, 2012–2013, *Ministry of the Environment, Japan, 2014*; **Paris**, 2009–2010, *Bressi et al., 2013*, No soil data; **Philadelphia**, 2013, *U.S. EPA chemical speciation network*; **Santiago**, 2013, *Villalobos et al., 2015*; **Sao Paulo**, 2008, *Souza et al., 2014*, No soil data; **Shanghai**, 2012–2013, *Shanghai EPB, 2014*; **Shenzhen**, 2013–2014, *Shenzhen EPB*, No soil data; **Singapore**, 2000, *Balasubramanian et al., 2003*, OM is calculated by weighted water-insoluble organic carbon and water-soluble organic carbon; No soil data; **Suzhou**, 2011–2012, *Cheng, 2013*; **Tianjin**, 2011, *Xu et al., 2015*; **Tokyo**, 2012–2013, *Ministry of the Environment, Japan, 2014*; **Toronto**, 2000–2001, Lee et al., 2003, Ti is calculated by [Al]/26.8 and Fe is calculated by [Al]/2.3; **Wuhan**, 2012–2013, *Zhang et al., 2015*, No soil data; **Xi'an**, 2010, *Wang et al., 2015*, Al, Si and Ca are calculated by [Fe]*2.3, [Fe]*8.8 and [Fe]*0.86, respectively. (For interpretation of the references to color in this figure legend, the reader is referred to the web version of this article.)

from 15% in Sao Paulo to 55% in Kitakyushu-Fukuoka. The minimum percentage for soil was 2% in London and the maximum was 26% in Tianjin. The "unidenfied" referred to unidentified $PM_{2.5}$ substances that also ranged from 2% in Cairo to 41% in Sao Paulo. The diversity was substantial due to different aerosol chemical characteristics across the world's megacities, which was also related to the collected data from the different studies, the different sampling devices and the analysis methods for each component.

The composition ratios among the megacities in the different $PM_{2.5}$ mass regions indicated the characteristics of the local emissions. For the 20 "non-attainment" megacities, the mass ratio in Delhi, Kolkata and Cairo was 51% for OM, 15% for EC, 17% for SNA, 11% for soil and 6% for unidentified, on average, which are notably different from those in the 13 Chinese megacities with 26% for OM, 5% for EC, 39% for SNA, 12% for soil and 18% for the unidentified, on average. The corresponding ratios in the 14 "target I-attainment" and "target II-attainment" megacities of Asia, America and Europe were 31% for OM, 9% for EC, 37% for SNA, 8% for soil and 15% for unidentified. For the eight "WHO-attainment" and "target III-attainment" megacities, all located in North America, the mass ratios were 30% for OM, 6% for EC, 34% for SNA, 7% for soil and 23% for unidentified. In general, carbonaceous substances dominated the Indian megacities and Cairo, and secondary inorganic aerosols were the most abundant composition for Chinese megacities. For the remaining megacities with relatively low $PM_{2.5}$ mass concentrations, organic carbonaceous substances were comparable and almost equal to that of secondary inorganic aerosols. The soil percentage of 11–12% in "non-attainment" megacities was slightly higher than the 7–8% in the remaining megacities, whereas the ratio of "unidentified" was between 12% and 23%, which is partially due to the underestimated organic matter contribution caused by the OC to OM conversion factor of 1.4 used in this study. More investigative work is expected for different locations to estimate a precise and local OM/OC converter (Turpin and Lim, 2001).

Source apportionment results further track the sources of these major $PM_{2.5}$ species in the representative megacities. For organic matter (OM), primary emissions still account for the majority measured in "non-attainment" megacities, from 65% in Beijing and 67% in Shanghai to 53% in Delhi (Guo et al., 2012; Shanghai EPB, 2014; Tiwari et al., 2013). Primary OM was largely emitted by diesel and gasoline vehicles, in addition to the burning of coal and biomass (Guo et al., 2012; Tiwari et al., 2013). However, secondary organic aerosols are not negligible and will keep rising after controlling for primary emissions. The dominant contribution of primary OM is also the case for the "target I-attainment" and "target II-attainment" megacities such as Santiago and Mexico City.

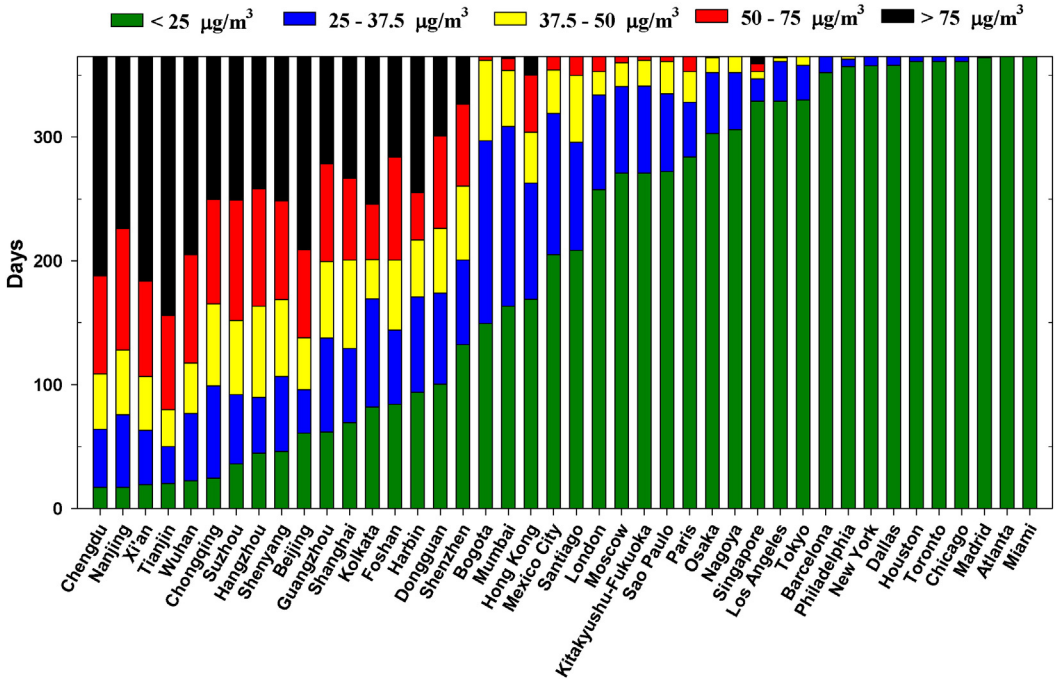

Fig. 5. Days separated by the threshold values of the WHO guideline. The threshold values of 25, 37.5, 50 and 75 μg/m^3 used for the daily concentration ranges are suggested by the guideline and interim targets I, II and III of the WHO. The megacities of Delhi, Cairo and Dhaka are excluded because the daily $PM_{2.5}$ concentrations are unavailable.

The SOA in Santiago could reach 54% in three warm months but decrease to almost zero in other months (Villalobos et al., 2015). The primary emission sources in Santiago are wood smoke (approximately 60% in cold months), diesel and gasoline vehicles (Villalobos et al., 2015). For Mexico City 54–79% of the OM is from primary emission sources (traffic emission: approximately 49% and wood smoke: 5–30%) (Stone et al., 2008). In contrast, secondary organic aerosols dominated the organic aerosols for the "WHO-attainment" and "target III-attainment" megacities. For New York, 70% of the OM is composed of secondary organic aerosols (SOA) and the remainder is from traffic and cooking (Sun et al., 2011). In Europe, the SOA accounts for 21–68% of the total carbon in winter and increases to 70–86% during the summer, which is typically a result of the volatile organic compounds from non-fossil fuel sources (Gelencsér et al., 2007). Over 80% of the SNA in the megacities of Beijing, Shanghai, Guangzhou and Chongqing was from the gaseous precursors emitted by power generation, industry and traffic, according to the chemical transport modeling results (Zhang et al., 2012a). The mass ratio of $[SO_4^{2-}]/[NO_3^-]$ is regarded as an indicator of the contribution weight of stationary sources such as power generation and traffic sources. To a certain extent, a higher $[SO_4^{2-}]/[NO_3^-]$ value signifies a greater percentage of sulfate oxidized from sulfur dioxide from stationary sources or regional upwind transport, and a lower value signifies a greater contribution of nitrogen oxides from both stationary and traffic sources. The $[SO_4^{2-}]/[NO_3^-]$ for the megacities of Kolkata (5.2), Atlanta (3.5), Cairo (3.2), Miami (3.0) and Delhi (2.8) were found to be much higher than Beijing (0.95), Shanghai (1.1), Guangzhou (1.9), Chicago (1.0), New York (1.1) and Toronto (1.2). Santiago (0.27), Los Angeles (0.5), Paris (0.7) and London (0.8) have the lowest $[SO_4^{2-}]/[NO_3^-]$ values, indicating the dominate contribution of traffic emissions (Bressi et al., 2013; Chowdhury, 2004; U.S. EPA chemical speciation network; Guangzhou EPB; Lee et al., 2003; Liu et al., 2015; Lowenthal et al., 2013; Shanghai EPB, 2014; Villalobos et al., 2015). However, it should also be noted that presence of ammonia also affects the $[SO_4^{2-}]/[NO_3^-]$ value, because ammonia is believed to be neutralized first by sulfuric acid to form ammonium sulfate or ammonium bisulfate and then the excess part of ammonia could react with nitric acid to form NH_4NO_3 and with hydrochloric acid to form NH_4Cl (McMurry et al., 1983).

3.3. Temporal evolution of polluted days

The polluted days exceeding the WHO daily threshold values in 2013 were counted for each megacity (shown in Fig. 5). Ranked by the polluted days exceeding the WHO daily guideline of 25 μg/m^3, the five megacities with the most number of polluted days were Chengdu (348 days), Nanjing (348 days), Xi'an (346 days) and Tianjin (345 days) in 2013. The five megacities with the least number of polluted days exceeding 25 μg/m^3 in 2013 were Toronto (4 days), Chicago (4 days), Madrid (1 day), Atlanta (0 day) and Miami (0 day). The days exceeding the daily WHO interim target I of 75 μg/m^3 ("non-attainment" days) all occurred in the megacities in Asia, varying from 6 in Singapore to 177 in Chengdu. For the number of days between the interim target II of 50 μg/m^3 and 75 μg/m^3 ("target I-attainment" days), the Asian megacities still comprise the majority, with an average of 48 days. The other megacities that had "target I-attainment" days were in America and Europe, from 1 day in Los Angeles to 15 days in Santiago. The "target II-attainment" days with a daily concentration between the interim target III of 37.5 μg/m^3 and 50 μg/m^3 occurred primarily in Asia and South America but occurred in a total of 34 global megacities. The "target II-attainment" days ranged from 2 in Philadelphia to 74 in Hangzhou, with an average of 39 days. The "target III-attainment" days with a daily concentration between the WHO guideline of 25 μg/m^3 and 37.5 μg/m^3 existed in all megacities except for Atlanta and Miami. The "target III-attainment" days were distributed almost evenly throughout Asia, South America and Europe, with an average of 53 days.

The polluted days exceeding the WHO daily threshold values, however, were not equally distributed throughout the year. Fig. 6 shows the monthly distribution for the polluted days in each megacity. For the "non-attainment" days with a concentration over 75 μg/m^3, December, January and February were the dominant months for all of the megacities, primarily in China and India, except during July in Singapore. Previous studies also indicated that winter was the peak $PM_{2.5}$ season in urban areas in China and India (Bisht et al., 2015; Chai et al., 2014; Cheng et al., 2013; Qu et al., 2010; Wang et al., 2014). The reasons for which are summarized in two folds. The first reason is the unfavorable dispersion conditions for pollutants in winter. A vertical temperature

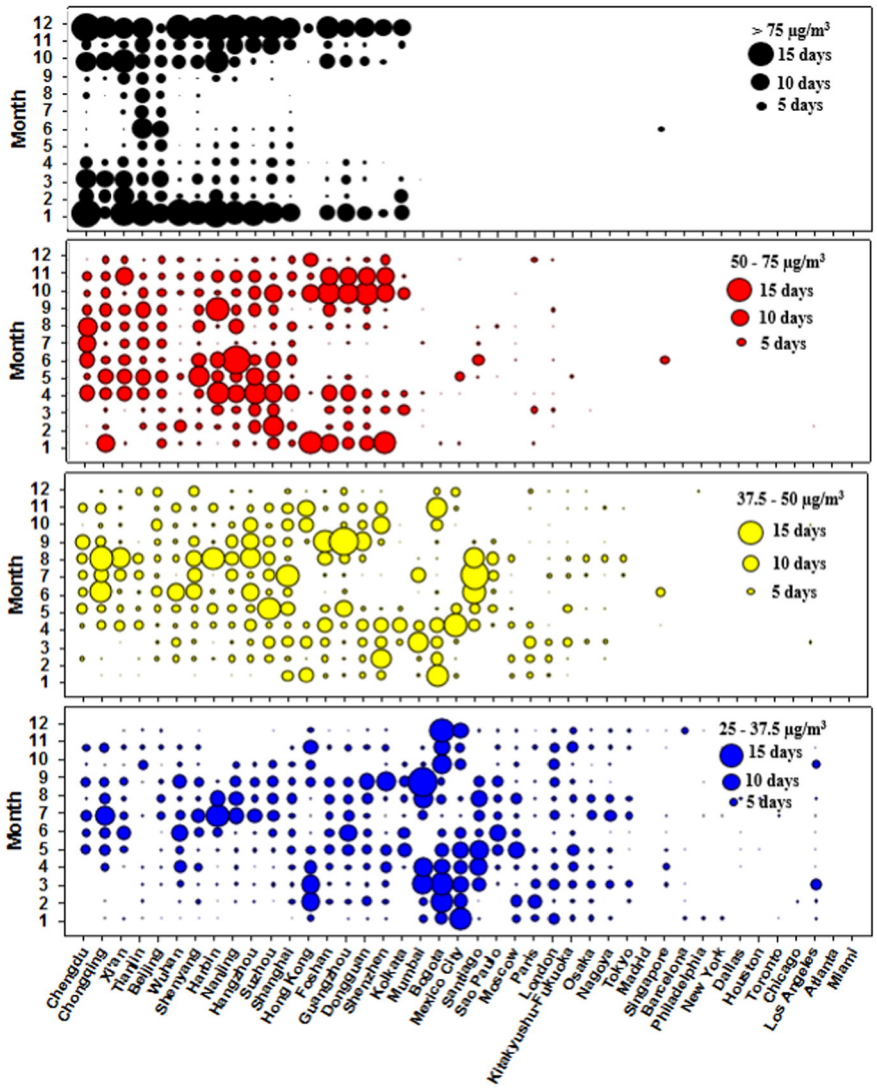

Fig. 6. Monthly distribution of the polluted days exceeding the WHO threshold values. The symbol size represents the number of polluted days for the corresponding month. The symbol color represents the different mass range. The megacities of Delhi, Dhaka and Cairo are excluded because only monthly or annual values are available. (For interpretation of the references to color in this figure legend, the reader is referred to the web version of this article.)

inversion was frequent in winter, accompanied by wind speeds less than 2 m/s and a mixing layer height less than 300 m (Huang et al., 2014a; Jiang et al., 2015). The second reason is the additional emission enhancement in winter. A heating season exists, usually from November to March, for the northern cities of China. Residential heating systems that burned coal increased SO_2 emissions as much as 24% at or near ground level (Hao et al., 2005). This is also true for Indian megacities that burned wood and agricultural waste to produce heat (Bisht et al., 2015). The heavy pollution occurring in July in Singapore was primarily caused by biomass burning in nearby Indonesia (Betha et al., 2014).

For the "target I-attainment" days with a concentration of 50–75 μg/m^3, although the polluted days were still present in the megacities of China, the peak months transferred to autumn (September, October and December), especially for southern China (i.e., Foshan, Donguan, Shenzhen and Hong Kong). April to June was also a period of high occurance of "target I-attainment" days for other megacities. Dust storms from Northern China (April), biomass burning after crop harvesting (May–June and October–November) and worsening dispersion conditions after summer likely accounted for the polluted days (Cheng et al., 2014; Fu et al., 2014; Hua et al., 2015). Eleven to fifteen polluted days were observed in May in Mexico City and in June in Santiago.

For the "target II-attainment" days with a concentration of 37.5–50 μg/m^3, the majority of these days in most megacities in China occurred in July, August and September, except for several megacities in southern China. Actually, the mass level of 37.5–50 μg/m^3 was a low level for the entire year, illustrating that summer and early autumn were seasons with clearer conditions for these Chinese megacities. Favorable dispersion conditions often occurred in summer when wind speeds and the mixing layer height were high and precipitation was abundant, especially for the coastal megacities influenced by the subtropical oceanic climate (Cheng et al., 2013). However, the majority of such favorable days in the megacities of southern China, Bogota and Mumbai were in the spring and autumn, between the most polluted winter season and clean summer season. In contrast, for Mexico City, Sao Paulo and Santiago, the autumn and winter months (April to August) are unfavorable for pollutant dispersion; stable conditions and thermal inversions are common and thresholds may be exceeded (de Miranda et al., 2012; Vega et al., 2011; Villalobos et al., 2015).

For the "target III-attainment" days with a concentration of 25–37.5 μg/m^3, the majority of Chinese megacities were limited to July and August, matching well with the summer season of these megacities, whereas the majority for the remaining southern Chinese megacities, Bogota and Mumbai occurred during February–April and August–

October. For Mexico City, Sao Paulo and Santiago, these polluted days were concentrated in February–May.

Overall, the meteorological conditions, such as thermal inversions occurred in winter, the elevated temperature for atmospheric oxidation in summer were the dominant factors that determined the seasonal variation of $PM_{2.5}$ mass in megacities. Additional emissions resulting from heating or open-air burning could also be enhanced during cold seasons. However, the climate system for each megacity was different and complex, as were the emission characteristics; the temporal pattern of polluted days was ultimately determined by the specific megacity, and the unique pattern was difficult to summarize.

4. Conclusions

This study intended to present a critical review of the $PM_{2.5}$ pollution status in global megacities. Based on the one-year official monitoring dataset of 2013, Delhi, India; Cairo, Egypt; and Xi'an, Tianjin and Chengdu, China, are the five megacities with the highest $PM_{2.5}$ annual average concentrations, ranging from 89 to 143 $\mu g/m^3$. The least polluted five megacities were Toronto, Canada; Miami, Philadelphia, and New York, United States; and Madrid, Spain, with a concentration between 7 and 10 $\mu g/m^3$. The $PM_{2.5}$ spatial distribution of the discrete megacities agreed well with the satellite-derivation distribution, indicating that the most polluted regions were concentrated in east-central China and the Indo-Gangetic Plain of Asia. The literature results showed that the organic matter and secondary inorganic ions (sulfate, nitrate and ammonium) composed the majority of the $PM_{2.5}$ mass, accounting for 30% and 36% of the total, respectively. A seasonal distribution of $PM_{2.5}$ polluted days existed due to meteorological conditions as well as an emission change in different seasons, especially for the polluted megacities in Asia.

There were 26 megacities without published $PM_{2.5}$ data for 2013. Most of these megacities are located in Asia, Africa and South America. The reasons might be due to the deficiency of $PM_{2.5}$ monitoring networks or lack of the transparency of measured data, indicating that the awareness of air pollution is still limited for the megacities in developing countries. Finally, a large disparity of $PM_{2.5}$ pollution levels existed between megacities in developing and developed countries. To address the $PM_{2.5}$ pollution situation in Asia, global collaboration between developed and developing megacities should be established and enhanced to optimize energy consumption structure and implement advanced emission-reducing technologies.

Acknowledgments

This work is supported by the Ministry of Environmental Protection's Special Funds for Research on Public Welfares (No. 201409002), the National Science and Technology Supporting Plan (No. 2014BAC22B01) and State Environmental Protection Key Laboratory of Sources and Control of Air Pollution Complex (No. SCAPC201409). We acknowledge Olga Kislova of Russian State Environmental Protection Institution, Rafael Borge of Technical University of Madrid, Néstor Y. Rojas of National University of Colombia, van Donkelaar of Dalhousie University and Jie Wang of Zhejiang University for their help with the data collection and process.

Appendix A. Supplementary data

Supplementary data to this article can be found online at http://dx.doi.org/10.1016/j.envint.2016.02.003.

References

Balasubramanian, R., Qian, W.B., Decesari, S., Facchini, M.C., Fuzzi, S., 2003. Comprehensive characterization of PM2.5 aerosols in Singapore. J. Geophys. Res.-Atmos. 108 (D16).

Betha, R., Behera, S.N., Balasubramanian, R., 2014. 2013 Southeast Asian smoke haze: fractionation of particulate-bound elements and associated health risk. Environ. Sci. Technol. 48 (8), 4327–4335.

Bisht, D.S., Dumka, U.C., Kaskaoutis, D.G., Pipal, A.S., Srivastava, A.K., Soni, V.K., et al., 2015. Carbonaceous aerosols and pollutants over Delhi urban environment: temporal evolution, source apportionment and radiative forcing. Sci. Total Environ. 521-522, 431–445.

Boys, B.L., Martin, R.V., van Donkelaar, A., MacDonell, R.J., Hsu, N.C., Cooper, M.J., et al., 2014. Fifteen-year global time series of satellite-derived fine particulate matter. Environ. Sci. Technol. 48 (19), 11109–11118.

Brauer, M., Amann, M., Burnett, R.T., Cohen, A., Dentener, F., Ezzati, M., et al., 2012. Exposure assessment for estimation of the global burden of disease attributable to outdoor air pollution. Environ. Sci. Technol. 46 (2), 652–660.

Bressi, M., Sciare, J., Ghersi, V., Bonnaire, N., Nicolas, J.B., Petit, J.E., et al., 2013. A one-year comprehensive chemical characterisation of fine aerosol ($PM_{2.5}$) at urban, suburban and rural background sites in the region of Paris (France). Atmos. Chem. Phys. 13 (15), 7825–7844.

Butler, T.M., Lawrence, M.G., Gurjar, B.R., van Aardenne, J., Schultz, M., Lelieveld, J., 2008. The representation of emissions from megacities in global emission inventories. Atmos. Environ. 42 (4), 703–719.

Chai, F., Gao, J., Chen, Z., Wang, S., Zhang, Y., Zhang, J., et al., 2014. Spatial and temporal variation of particulate matter and gaseous pollutants in 26 cities in China. J. Environ. Sci. 26 (1), 75–82.

Chen, P.L., Wang, T.J., Hu, X., Xie, M., Zhuang, B.L., Li, S., 2015a. A study of chemical mass balance source apportionment of fine particulate matter in Nanjing. J. Nanjing Univ. (Nat. Sci.) 51 (3), 524–534.

Chen, Y., Xie, S.D., Luo, B., 2015b. Composition and pollution characteristics of fine particles in Chengdu during 2012 to 2013. Acta Sci. Circumst. http://dx.doi.org/10.13671/j.hjkxxb.2015.0501.

Cheng, Z., 2013. Relationship between haze pollution and aerosol properties in the Yangtze River Delta of China (Doctoral Dissertation) Tsinghua University.

Cheng, Z., Jiang, J., Fajardo, O., Wang, S., Hao, J., 2013. Characteristics and health impacts of particulate matter pollution in China (2001−2011). Atmos. Environ. 65, 186–194.

Cheng, Z., Wang, S., Fu, X., Watson, J.G., Jiang, J., et al., 2014. Impact of biomass burning on haze pollution in the Yangtze River delta, China: a case study in summer 2011. Atmos. Chem. Phys. 14 (9), 4573–4585.

Chow, J.C., Doraiswamy, P., Watson, J.G., Antony-Chen, L.W., Ho, S.S.H., et al., 2008. Advances in integrated and continuous measurements for particle mass and chemical, composition. J. Air Waste Manage. Assoc. 58 (2), 141–163.

Chow, J.C., Lowenthal, D.H., Chen, L.W., Wang, X., Watson, J.G., 2015. Mass reconstruction methods for PM2.5: a review. Air Qual. Atmos. Health 8 (3), 243–263.

Chowdhury, M., 2004. Characterization of fine particle air pollution in the Indian subcontinent (Ph.D. Thesis) Georgia Institute of Technology, USA.

Day, M.C., Zhang, M., Pandis, S.N., 2015. Evaluation of the ability of the EC tracer method to estimate secondary organic carbon. Atmos. Environ. 112, 317–325.

de Miranda, R.M., de Fatima Andrade, M., Fornaro, A., Astolfo, R., de Andre, P.A., Saldiva, P., 2012. Urban air pollution: a representative survey of $PM_{2.5}$ mass concentrations in six Brazilian cities. Air Qual. Atmos. Health 5 (1), 63–77.

Fu, X., Wang, S.X., Cheng, Z., Xing, J., Zhao, B., Wang, J.D., et al., 2014. Source, transport and impacts of a heavy dust event in the Yangtze River Delta, China, in 2011. Atmos. Chem. Phys. 14 (3), 1239–1254.

Gelencsér, A., May, B., Simpson, D., Sánchez-Ochoa, A., Kasper-Giebl, A., et al., 2007. Source apportionment of PM2.5 organic aerosol over Europe: Primary/secondary, natural/anthropogenic, and fossil/biogenic origin. J. Geophys. Res. Atmos. 112 (D23) (1984–2012).

Guangzhou Environmental Protection Bureau (EPB). http://finance.sina.com.cn/china/dfjj/20150420/061021994918.shtml. Last accessed 2015.07.26)

Guo, S., Hu, M., Guo, Q., Zhang, X., Zheng, M., Zheng, J., et al., 2012. Primary sources and secondary formation of organic aerosols in Beijing, China. Environ. Sci. Technol. 46 (18), 9846–9853.

Gurjar, B.R., Jain, A., Sharma, A., Agarwal, A., Gupta, P., Nagpure, A.S., et al., 2010. Human health risks in megacities due to air pollution. Atmos. Environ. 44 (36), 4606–4613.

Hao, J.M., Wang, L.T., Li, L., Hu, J.N., Yu, X.C., 2005. Air pollutants contribution and control strategies of energy-use related sources in Beijing. Sci. China Ser. D Earth Sci. 48, 138–146.

Hara, K., Homma, J., Tamura, K., Inoue, M., Karita, K., Yano, E., 2013. Decreasing trends of suspended particulate matter and PM2.5concentrations in Tokyo, 1990–2010. J. Air Waste Manage. Assoc. 63 (6), 737–748.

Hasheminassab, S., Daher, N., Ostro, B.D., Sioutas, C., 2014. Long-term source apportionment of ambient fine particulate matter (PM2.5) in the Los Angeles Basin: a focus on emissions reduction from vehicular sources. Environ. Pollut. 193, 54–64.

Hua, Y., Cheng, Z., Wang, S., Jiang, J., Chen, D., et al., 2015. Characteristics and source apportionment of $PM_{2.5}$ during a fall heavy haze episode in the Yangtze River Delta of China. Atmos. Environ. 123 (B), 380–391.

Huang, K., Zhuang, G., Wang, Q., Fu, J.S., Lin, Y., Liu, T., et al., 2014a. Extreme haze pollution in Beijing during January 2013: chemical characteristics, formation mechanism and role of fog processing. Atmos. Chem. Phys. Discuss. 14 (6), 7517–7556.

Huang, X.H., Bian, Q.J., Ng, W.M., Louie, P.K., Yu, J.Z., 2014b. Characterization of $PM_{2.5}$ Major Components and source investigation in suburban Hong Kong: a one year monitoring study. Aerosol Air Qual. Res. 14, 237–250.

Huang, Y., Shen, H., Chen, H., Wang, R., Zhang, Y., Su, S., et al., 2014c. Quantification of global primary emissions of $PM_{2.5}$, PM_{10}, and TSP from combustion and industrial process sources. Environ. Sci. Technol. 48 (23), 13834–13843.

IPCC, 2013. The Fifth Assessment Report of the Intergovernmental Panel on Climate Change. United Kingdom and New York, NY, USA, Cambridge.

Jia, L.L., 2014. Study on Pollution Characteristics and Source Apportionment of Atmospheric Particles on the Northern Cold Northern Cold Region (Master Thesis) Harbin Institute of Technology.

Jiang, J., Zhou, W., Cheng, Z., Wang, S., He, K., Hao, J., 2015. Particulate matter distributions in China during a winter period with frequent pollution episodes (January 2013). Aerosol Air Qual. Res. 15 (2), 494–503.
Joseph, A.E., Seema, U., Rakesh, K., 2012. Chemical characterization and mass closure of fine aerosol for different land use patterns in Mumbai City. Aerosol Air Qual. Res. 12, 61–72.
Kan, H., Chen, R., Tong, S., 2012. Ambient air pollution, climate change, and population health in China. Environ. Int. 42, 10–19.
Klimont, Z., Smith, S.J., Cofala, J., 2013. The last decade of global anthropogenic sulfur dioxide: 2000–2011 emissions. Environ. Res. Lett. 8 (1), 014003.
Lee, P.K.H., Brook, J.R., Dabek-Zlotorzynska, E., Mabury, S.A., 2003. Identification of the Major Sources contributing to PM2.5 observed in Toronto. Environ. Sci. Technol. 37 (21), 4831–4840.
Lin, J., Pan, D., Davis, S.J., Zhang, Q., He, K., Wang, C., et al., 2014. China's international trade and air pollution in the United States. Proc. Natl. Acad. Sci. 111 (5), 1736–1741.
Liu, B.X., Zhang, D.W., Chen, T., Yang, D.Y., Yang, L., Chang, M., et al., 2015. Analysis of the characteristics and major chemical compositions of $PM_{2.5}$ in Beijing. Acta Sci. Circumst. http://dx.doi.org/10.13671/j.hjkxxb.2015.0131.
Lowenthal, D., Naresh, K., 2003. $PM_{2.5}$ mass and light extinction reconstruction in IMPROVE. J. Air Waste Manage. Assoc. 53 (9), 1109–1120.
Lowenthal, D.H., Gertler, A.W., Labib, M.W., 2013. Particulate matter source apportionment in Cairo: recent measurements and comparison with previous studies. Int. J. Environ. Sci. Technol. 11 (3), 657–670.
Madrigano, J., Kloog, I., Goldberg, R., Coull, B.A., Mittleman, M.A., Schwartz, J., 2013. Long-term exposure to PM2.5 and incidence of acute myocardial infarction. Environ. Health Perspect. 121 (2), 192–196.
McMurry, P.H., Takano, H., Anderson, G.R., 1983. Study of the ammonia (gas)-sulfuric acid (aerosol) reaction rate. Environ. Sci. Technol. 17 (6), 347–352.
Ministry of the Environment, Japan, 2014. Measurement data of $PM_{2.5}$ in Japanese fiscal year 2012. https://www.env.go.jp/air/osen/pm/monitoring/data/h24.html.
Philip, S., Martin, R.V., van Donkelaar, A., Lo, J.W., Wang, Y., Chen, D., et al., 2014. Global chemical composition of ambient fine particulate matter for exposure assessment. Environ. Sci. Technol. 48 (22), 13060–13068.
Qu, W.J., Arimoto, R., Zhang, X.Y., Zhao, C.H., Wang, Y.Q., Sheng, L.F., et al., 2010. Spatial distribution and interannual variation of surface PM_{10} concentrations over eighty-six Chinese cities. Atmos. Chem. Phys. 10 (12), 5641–5662.
Rodriguez, S., van Dingenen, R., Putaud, J.P., Dell'Acqua, A., Pey, J., Querol, X., et al., 2007. A study on the relationship between mass concentrations, chemistry and number size distribution of urban fine aerosols in Milan, Barcelona and London. Atmos. Chem. Phys. 7 (9), 2217–2232.
Shanghai Environmental Protection Bureau (EPB), 2014. Source Apportionment of Ambient Fine Particulate Matter for Shanghai City (Report).
Shenzhen Environmental Protection Bureau (EPB). http://www.sznews.com/news/content/2015-04/28/content_11519429.htm?prolongation=1. (Last accessed 2015.07.26)
Souza, D.Z., Vasconcellos, P.C., Lee, H., Aurela, M., Saarnio, K., et al., 2014. Composition of PM2.5 and PM10 collected at urban sites in Brazil. Aerosol Air Qual. Res. 14, 168–176.
Stone, E.A., Snyder, D.C., Sheesley, R.J., Sullivan, A., Weber, R., Schauer, J., 2008. Source apportionment of fine organic aerosol in Mexico City during the MILAGRO experiment 2006. Atmos. Chem. Phys. 8 (5), 1249–1259.
Sun, Y.L., Zhang, Q., Schwab, J.J., Demerjian, K.L., Chen, W.N., Bae, M.S., et al., 2011. Characterization of the sources and processes of organic and inorganic aerosols in New York City with a high-resolution time-of-flight aerosol mass spectrometer. Atmos. Chem. Phys. 11 (4), 1581–1602.
Taylor, S.R., McLennan, S.M., 1995. The geochemical evolution of the continental crust. Rev. Geophys. 33 (2), 241–265.
Tiwari, S., Srivastava, A.K., Bisht, D.S., Safai, P.D., Parmita, P., 2013. Assessment of carbonaceous aerosol over Delhi in the Indo-Gangetic Basin: characterization, sources and temporal variability. Nat. Hazards 65 (3), 1745–1764.
Turpin, B.J., Lim, H., 2001. Species contributions to $PM_{2.5}$ mass concentrations: revisiting common assumptions for estimating organic mass. Aerosol Sci. Technol. 35 (1), 602–610.
United Nations, 2014. World Urbanization Prospects: Highlights (the 2014 Revision). (http://esa.un.org/unpd/wup/Highlights/WUP2014-Highlights.pdf).
United States Environmental Protection Agency (EPA), Chemical Speciation Network. https://www.sdas.battelle.org/CSNAssessment/html/Default.html. Last access:2016-02-05
van Donkelaar, A., Martin, R.V., Brauer, M., Boys, B.L., 2015. Use of satellite observations for long-term exposure assessment of global concentrations of fine particulate matter. Environ. Health Perspect. 123 (2), 135–143.
Vega, E., Ruiz, H., Escalona, S., Cervantes, A., Lopez-Veneroni, D., Gonzalez-Avalos, et al., 2011. Chemical composition of fine particles in Mexico City during 2003–2004. Atmos. Pollut. Res. 2 (4).
Villalobos, A.M., Barraza, F., Jorquera, H., Schauer, J.J., 2015. Chemical speciation and source apportionment of fine particulate matter in Santiago, Chile, 2013. Sci. Total Environ. 512–513, 133–142.
Wang, Y., Ying, Q., Hu, J., Zhang, H., 2014. Spatial and temporal variations of six criteria air pollutants in 31 provincial capital cities in China during 2013–2014. Environ. Int. 73, 413–422.
Wang, P., Cao, J.J., Shen, Z.X., Han, Y.M., Lee, S.C., Huang, Y., et al., 2015. Spatial and seasonal variations of $PM_{2.5}$ mass and species during 2010 in Xi'an, China. Sci. Total Environ. 508, 477–487.
World Health Organization, 2006. Air quality guidelines: global update 2005. Particulate Matter, Ozone, Nitrogen Dioxide and Sulfur Dioxide (http://whqlibdoc.who.int/hq/2006/WHO_SDE_PHE_OEH_06.02_eng.pdf?ua=1).
World Health Organization, 2014. Ambient (outdoor) air pollution in cities database. (http://www.who.int/phe/health_topics/outdoorair/databases/cities/en/).
Xu, H., Bi, X.H., Zheng, W.W., Wu, J.H., Feng, Y.C., 2015. Particulate matter mass and chemical component concentrations over four Chinese cities along the western Pacific coast. Environ. Sci. Pollut. Res. Int. 22 (3), 1940–1953.
Yang, F., Tan, J., Zhao, Q., Du, Z., He, K., Ma, Y., et al., 2011. Characteristics of $PM_{2.5}$ speciation in representative megacities and across China. Atmos. Chem. Phys. 11 (11), 5207–5219.
Yu, L.D., Wang, G.F., Zhang, R.J., Zhang, L.M., Song, Y., Wu, B.B., et al., 2013. Characterization and source apportionment of $PM_{2.5}$ in an Urban Environment in Beijing. Aerosol Air Qual. Res. 13 (2), 574–583.
Zhang, H., Li, J., Ying, Q., Yu, J.Z., Wu, D., Cheng, Y., et al., 2012a. Source apportionment of $PM_{2.5}$ nitrate and sulfate in China using a source-oriented chemical transport model. Atmos. Environ. 62, 228–242.
Zhang, X.Y., Wang, Y.Q., Niu, T., Zhang, X.C., Gong, S.L., Zhang, Y.M., et al., 2012b. Atmospheric aerosol compositions in China: spatial/temporal variability, chemical signature, regional haze distribution and comparisons with global aerosols. Atmos. Chem. Phys. 12 (2), 779–799.
Zhang, F., Wang, Z.W., Cheng, H.R., Lv, X.P., Gong, W., Wang, X.M., et al., 2015. Seasonal variations and chemical characteristics of $PM_{2.5}$ in Wuhan, Central China. Sci. Total Environ. 518-519, 97–105.